

# Effective Theory of Ultrafast Skyrmion Nucleation

Rein Liefferink,<sup>1,\*</sup> Lukas Körber,<sup>1</sup> Kathinka Gerlinger,<sup>2</sup> Bastian Pfau,<sup>2</sup> Felix Büttner,<sup>3,4</sup> and Johan H. Mentink<sup>1,†</sup>

<sup>1</sup>*Radboud University, Institute of Molecules and Materials,  
Heyendaalseweg 135, 6525 AJ Nijmegen, The Netherlands*

<sup>2</sup>*Max Born Institute for Nonlinear Optics and Short Pulse Spectroscopy, 12489 Berlin, Germany*

<sup>3</sup>*Helmholtz-Zentrum Berlin für Materialien und Energie, 14109 Berlin, Germany*

<sup>4</sup>*Experimental Physics V, Center for Electronic Correlations and Magnetism, University of Augsburg, 86159 Augsburg, Germany*

(Dated: April 16, 2025)

Laser-induced ultrafast skyrmion nucleation has been experimentally demonstrated in several materials. So far, atomistic models have been used to corroborate experimental results. However, such simulations do not provide a simple intuitive understanding of the underlying physics. Here, we propose a coarse-grained effective theory where skyrmions can be nucleated or annihilated by thermal activation over energy barriers. Evaluating these two processes during a heat pulse shows good agreement with atomistic spin dynamics simulations and experiments while drastically reducing computational complexity. Furthermore, the effective theory provides a direct guide for experimentally optimizing the number of nucleated skyrmions. Interestingly, the model also predicts a novel pathway for ultrafast annihilation of skyrmions. Our results pave the way for a deeper understanding of ultrafast nanomagnetism and the role of non-equilibrium physics.

**Introduction** — Pushing the limits for writing magnetic bits to ever smaller length and time scales is a fundamental challenge in magnetism that can have profound impact on magnetic data storage technology. Following pioneering studies on single-pulse all-optical switching (AOS) in ferrimagnetic GdFeCo [1], AOS was discovered in a wide range of ferrimagnets [2–4] and found to be well understood within an effective phenomenological theory [5, 6], which classifies different regimes of ultrafast spin dynamics depending on the transient electron temperature profile. As a result, tuning this profile enabled ultrafast write/erase cycles [7–10]. On the nanoscale, AOS was studied using femtosecond x-ray spectroscopies [11, 12] and spatially inhomogeneous excitation with transient X-ray gratings [13, 14] that allow spatial shaping of the electron temperature distribution. This led to the discovery of nanoscale AOS in ferrimagnets [15].

In ferromagnets, deterministic switching has been achieved with trains of several pulses. Following the first studies on CoPt thin films [16–18], phenomenological models have been developed for granular FePt systems [19, 20], which have recently been generalized to explain magnetic force microscopy measurements of stochastic switching of nanoscale domains in CoPt films [21]. The models and experiments, however, indicate that this pathway does not support deterministic single-pulse AOS and it remains an open question whether such switching is feasible for ferromagnets in principle [19–25].

In recent breakthrough experiments, a different form of ultrafast single-pulse switching has been demonstrated in related ferromagnetic systems hosting magnetic skyrmions [26–30] – highly localized nanoscale swirling textures in the magnetization that exhibit great stability and tunability. These phenomena offer an appealing alternative approach to investigate ultrafast writing of magnetic domains on the nanoscale. One of the defining properties of skyrmions is that their mag-

netization profile  $\mathbf{m}(\mathbf{r})$  has unit topological charge

$$N = \frac{1}{4\pi} \int_S \mathbf{m} \cdot \left( \frac{\partial \mathbf{m}}{\partial x} \times \frac{\partial \mathbf{m}}{\partial y} \right) dx dy = \pm 1, \quad (1)$$

where the sign is determined by the type of skyrmion and the orientation of the  $z$ -axis (assuming a skyrmion in  $xy$ -plane), which is typically the same for all skyrmions in a system. In particular, when the area of integration  $S$  contains several skyrmions, the number  $N$  also represents the number of skyrmions.

So far, atomistic spin dynamics (ASD) simulations have proven crucial in understanding these ultrafast skyrmion nucleation results, providing excellent qualitative agreement with key experimental signatures [28]. However, limited by the heavy computational costs, modeling realistic system sizes or including long-range interactions to achieve accurate time and length scales of skyrmion dynamics are until now out of reach. Moreover, no effective phenomenological theory of ultrafast nucleation of magnetic skyrmions has been reported so far. In particular, an intuitive description of the dependencies on external parameters like magnetic field and electron temperature profile is missing and very hard to extract from atomistic models featuring tens of thousands degrees of freedom.

The most notable existing effective models of skyrmions feature collective variables approaches within micromagnetism, the continuum counterpart of ASD. Most famously, the Thiele equation

$$\frac{\partial \mathbf{X}}{\partial t} \times \mathbf{G} + \alpha_G \hat{D} \frac{\partial \mathbf{X}}{\partial t} = \mathbf{F} \quad (2)$$

emerges by assuming a stable skyrmion profile  $\mathbf{m}(\mathbf{r}, t) = \mathbf{m}_0(\mathbf{r} - \mathbf{X}(t))$  parametrized by a center-of-mass position  $\mathbf{X}(t) = (x(t), y(t))$  and integrating out all other degrees of freedom [31, 32]. Here,  $\mathbf{G} = 4\pi\mu_0 N M_s d / \gamma \cdot \hat{\mathbf{z}}$  is the gyrovector ( $M_s$  is the saturation magnetization,  $\gamma$  is the gyromagnetic ratio,  $d$  the thickness of the sample), while  $\alpha_G$  is the Gilbert damping factor and  $\hat{D}$  the dissipation tensor. The

\* rein.liefferink@ru.nl

† johan.mentink@ru.nl

right-hand side  $\mathbf{F}$  may contain effective forces due to repulsion from a boundary or by other skyrmions and drag by field gradients, spin-polarized currents, or scattering with magnons [33]. Similar to the center-of-mass motion, deformation of the skyrmion shape may also be described using collective variables. Nevertheless, despite its wide applicability, this type of theory cannot be easily generalized to the ultrafast regime. Apart from the fact that dynamics according to the Thiele equation with time scales of nanoseconds [34] are comparatively slow, an even more fundamental obstacle is that Eq. (2) conserves the skyrmion number  $N$ . In other words, creation and annihilation events cannot be described.

In this Letter, we propose a new effective theory for ultrafast skyrmion dynamics in the regime complimentary to where the Thiele equation is valid, shaded turquoise in Fig. 1. The key dynamical variable here is the skyrmion number  $N = N(t)$ , while the skyrmion positions  $\mathbf{X}_i$  are (approximately) constant. The magnetic system in this regime does not evolve through continuous movements, but only by skyrmion nucleation and annihilation events. These fluctuations are individually highly localized in space, allowing for a simple mathematical description where skyrmions are treated as statistically independent hard disks. A simple probabilistic theory based on activation over an energy barrier according to the Arrhenius law then allows us to obtain the evolution of the ensemble average  $\langle N \rangle$ . The resulting theory captures previously reported results of skyrmion nucleation by a heat pulse, but also predicts new scenarios of laser-induced skyrmion annihilation that are in excellent agreement with atomistic simulations. Hence, this theory expands the understanding of ultrafast magnetism at the nanoscale and allows designing new experiments in ultrafast nanomagnetism.

The remainder of this letter is structured as follows. First, we provide estimates for interaction pathways between skyrmions. We use this to map out a sizable space-time region where nucleation and decay events are approximately independent, defining the regime of validity of the theory. Second, we derive a kinetic theory for skyrmion number  $\langle N(t) \rangle$  using the independence and consider its results for different temperature profiles. Third, we confirm predictions from the second part with atomistic simulations. Finally, we discuss implications and draw conclusions.

In the absence of strong thermal gradients, field gradients or spin currents, skyrmion motion is dominated by thermal diffusion. Breathing and other vibrational modes may also be thermally excited, but these can be neglected as they do not contribute to center-of-mass motions. In most skyrmion-hosting materials significant pinning occurs [35–37]. To obtain an upper bound on skyrmion diffusion, we first consider idealized free diffusion of a high-quality low-damping material. Typical material parameters are a Gilbert-damping factor on the order of  $\alpha_G = 0.01$ , samples with a magnetic layer thickness around  $d = 10$  nm and saturation magnetization around  $M_s = 1.1$  MA/m at room temperature  $T = 300$  K [38, 39]. The coefficient of free diffusion can then be calculated using the Thiele equation. In the Belavin-Polyakov limit

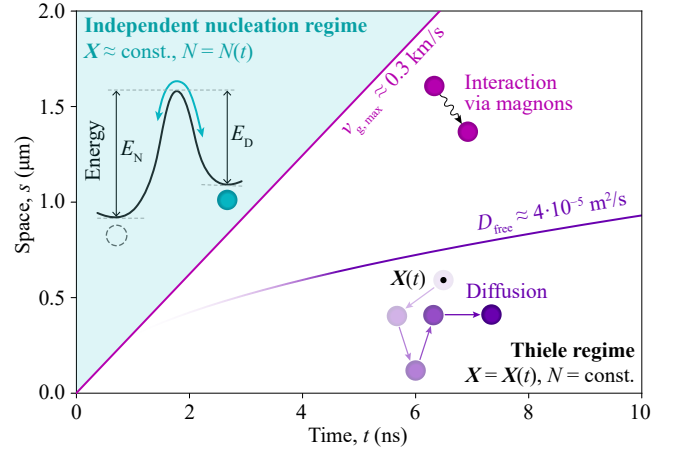


Figure 1. Space-time diagram of skyrmion dynamics illustrating the regime of validity of the presented theory for nucleation and decay of non-interacting skyrmions. Slow dynamics like changes in their position  $\mathbf{X}(t)$  by free diffusion are governed by the Thiele equation that preserves the skyrmion number  $N$ . Long-range interactions between skyrmions are limited by the maximum group velocity  $v_{g,\max}$  of the magnons that can efficiently scatter with skyrmions (see text for the estimation of  $D_{\text{free}}$  and  $v_{g,\max}$ ). Thus, outside of the magnon “light cone”, the positions  $\mathbf{X} \approx \text{const.}$  and nucleation/decay dynamics of  $N(t)$  can be assumed as independent activation events over an energy barrier.

[32, 40, 41], we can approximate it as (details in Appendix A)

$$D_{\text{free}} = k_B T \frac{1}{G} \frac{\alpha_G}{1 + \alpha_G^2} \approx 4 \cdot 10^{-5} \text{ m}^2/\text{s}. \quad (3)$$

Note that this approach breaks down at very short time scales since the effects of defects become larger and magnons and precession come into play (e.g. Walker breakdown). Clearly this calculation provides an upper bound for skyrmion diffusion, with experimentally determined values being orders of magnitude lower than  $D_{\text{free}}$  [36, 37].

The corresponding space-time regime is shown in Fig. 1, being limited by the distance  $s = \sqrt{2D_{\text{free}}t}$  covered during free diffusion. Outside of this regime, short-range interactions (e.g. repulsion) between different skyrmions are strongly suppressed. Long-range interactions mediated by magnons are, in return, limited by their maximum group velocity  $v_{g,\max}$ . As shown in Appendix B, we estimate an upper bound for the velocity of magnons that can scatter with skyrmions and therefore mediate long-range interactions as

$$v_{g,\max} = 8\gamma \frac{A_{\text{ex}}}{M_s} \frac{1}{R} \approx 0.3 \text{ km/s}, \quad (4)$$

where we assert  $A_{\text{ex}} = 12$  pJ/m as a typical micromagnetic exchange stiffness constant and  $R \approx 50$  nm as the skyrmion radius [28, 38, 39]. As shown in Fig. 1, this defines a region of space-like separation outside of the magnonic light cone  $s = v_{g,\max}t$  where the skyrmion positions  $\mathbf{X} \approx \text{const.}$  and interaction between skyrmions is negligible. We note that magnons in typical skyrmion materials can be strongly attenuated, effectively enlarging the non-interacting regime.

*Effective theory* — We proceed to construct a kinetic equation for the topological charge  $N(t)$  that can only change through nucleation or annihilation of individual skyrmions. Within the aforementioned space-time regime of non-interacting skyrmions, these nucleation and annihilation events can be treated as statistically independent, which allows to substantially simplify our model.

At finite temperature, the number of skyrmions  $N$  is a stochastic quantity. Therefore, we sum over all possible microstates  $i$  (i.e. configurations of skyrmions) to obtain the ensemble average

$$\langle N \rangle = \sum_{i \in \text{all microstates}} P_i N_i \quad (5)$$

with  $P_i$  and  $N_i$  respectively being the probability of finding the system in the microstate  $i$  and the number of skyrmions in this microstate. We can obtain microstates using the discussed independence by coarse-graining the sample into  $N_{\max}$  statistically equivalent regions such that each one can host exactly one skyrmion. It now follows that a microstate  $i$  with  $N$  skyrmion has probability  $P_i = p^N (1-p)^{N_{\max}-N}$ , where  $p$  is the chance to find a skyrmion in a single region. Microstates with  $N_i = N$  are obtained by choosing  $N$  regions with a skyrmion out of  $N_{\max}$ , which can be done in  $\binom{N_{\max}}{N}$  ways. Hence,

$$\langle N \rangle = \sum_{N=0}^{N_{\max}} \binom{N_{\max}}{N} p^N (1-p)^{N_{\max}-N} N = p N_{\max}. \quad (6)$$

In particular, the full distribution of the stochastic variable  $N$  is binomial with probability  $p$  over  $N_{\max}$  samples. This may be expected since we are dealing with  $N_{\max}$  independent binary systems with probabilities  $p$ . The problem is now reduced to finding a kinetic equation for the local variable  $p$ .

In the simplest case, a given skyrmion-supporting region can be either in a homogeneous magnetization state or skyrmion state. In a time interval  $dt$ , transitions between these states in either direction can lead to a change  $dp$  of  $p$ . We can write

$$dp = (dp)_{\text{nuc}} - (dp)_{\text{dec}}, \quad (7)$$

where  $(dp)_{\text{nuc}}$  and  $(dp)_{\text{dec}}$  are the respective probability of transition towards and from the skyrmion state, that is a nucleation or decay event, within  $dt$ . A skyrmion with lifetime  $\tau_D$  has a chance  $dt/\tau_D$  to decay during  $dt$ . This can only happen if a skyrmion is present, which has probability  $p$ , so  $(dp)_{\text{dec}} = p dt/\tau_D$ . Nucleation is only possible in the absence of a skyrmion, leading to  $(dp)_{\text{nuc}} = (1-p)dt/\tau_N$ , where  $\tau_N$  the nucleation time (or lifetime of the empty state). Assuming the independence of nucleation and decay processes, we can combine this into a differential equation

$$\frac{dp}{dt} = \frac{1-p}{\tau_N} - \frac{p}{\tau_D}. \quad (8)$$

Here we focus on transitions induced by thermal fluctuations, so time scales  $\tau_N$  and  $\tau_D$  are a function of temperature  $T$ . Temperature-driven skyrmion nucleation and especially decay have been studied in great detail, experimentally [42, 43], within micromagnetism [38, 44–46], atomistic

spin dynamics [47–49] and transition state theory [50, 51]. The most commonly used model is Arrhenius-type activation over the energy barrier between the empty and skyrmion state [42, 47, 50–54], in which

$$\tau_i = \tau_{0,i} \exp\left(\frac{E_i}{k_B T}\right) \text{ with } i = N, D, \quad (9)$$

where  $\tau_{0,N}$  and  $\tau_{0,D}$  are so-called attempt times and  $T$  is the temperature. The nucleation energy barrier  $E_N$  is the difference between the empty state and the top of the barrier, while the decay energy  $E_D$  is given by the top of the barrier compared to the skyrmion state (see Fig. 1 inset). Determination of these energy barriers and attempt times, including their possible temperature dependencies, can be challenging in general [38, 42, 44, 47, 50–54]. However, to understand the physics of our kinetic equation, only the strong temperature dependence due to the exponential function is important.

The kinetic equation of the expectation value  $\langle N \rangle = N_{\max} p$  now directly follows by multiplying both sides of Eq. (8) with  $N_{\max}$

$$\frac{d\langle N \rangle}{dt} = \frac{N_{\max} - \langle N \rangle}{\tau_N} - \frac{\langle N \rangle}{\tau_D}, \quad (10)$$

providing the central equation of the effective theory.

While the form of Eq. (10) is more transparent to its physical origin, it is equivalent to the mathematically simpler

$$\frac{d\langle N \rangle}{dt} = \frac{N_{\max}}{\tau_N} - \left(\frac{1}{\tau_N} + \frac{1}{\tau_D}\right) \langle N \rangle = -\frac{\langle N \rangle - N_{\text{eq}}}{\tau_R}, \quad (11)$$

where  $1/\tau_R = 1/\tau_D + 1/\tau_N$  and  $N_{\text{eq}} = N_{\max} \tau_R / \tau_N$ . That is, the kinetic equation for  $\langle N \rangle$  describes the exponential relaxation towards an instantaneous equilibrium value  $N_{\text{eq}}$  with a response time  $\tau_R$ . In particular, if the rates are constant, e.g., at constant temperature, one has

$$\langle N(t) \rangle = \langle N(0) \rangle + [N_{\text{eq}} - \langle N(0) \rangle] (1 - e^{-t/\tau_R}). \quad (12)$$

Due to its simplicity, various scenarios for ultrafast control of the number of skyrmions  $\langle N \rangle$  emerge directly from the effective theory Eq. (11). The most obvious control is based on tuning the transient temperature profile  $T(t)$ , as was done for the AOS in ferrimagnets. Experimentally, temperature profiles are achieved using ultrashort laser (or current pulses for longer time scales), which can be tuned using fluence, pulse width and sample heat dissipation properties [3, 7, 9, 10, 14, 28].

As an illustration, we assert Arrhenius time scales with temperature-independent energy barriers  $E_D = 0.7 E_N$  and attempt times  $\tau_{D,0} = \tau_{N,0} = \tau_0$  for decay and nucleation, respectively. This case where the skyrmions do *not* constitute the ground state, is particularly interesting, since we will see that it is nevertheless possible to generate and stabilize them. To keep the parameters of the temperature profile  $T(t)$  minimal, we chose a rectangular heat pulse with base temperature  $T_0 = 0.05 E_N/k_B$ , height  $T_p = 0.4 E_N/k_B$  and width  $w_0 = 15\tau_0$ , followed by an exponential cooling with

rate  $\tau_{\text{cool}}$ . The pulse shapes for different  $\tau_{\text{cool}}$  are shown in Fig. 2(a), along with the resulting evolutions of the skyrmion number  $\langle N \rangle$  in Fig. 2(b).

During the initial heating period at high constant temperature, skyrmions are rapidly nucleated and follow the simple exponential growth Eq. (12). Remarkably, when the temperature pulse is turned off instantly after the heating period (where  $\tau_{\text{cool}} \ll \tau_0$ ), the skyrmion number is "frozen in" and remains almost constant within the considered time scale. This can be understood by the strong temperature dependence of both the instantaneous equilibrium level  $N_{\text{eq}}$  and the response time  $\tau_R$  shown in Fig. 2(c) and Fig. 2(d), respectively. Naturally, at high temperatures, spontaneous activation over the skyrmion nucleation energy barrier becomes more likely, increasing the expected occupation of the skyrmion states  $N_{\text{eq}}$ . Along with the nucleation and decay time, the response time  $\tau_R$  is even more strongly affected by the increase in temperature, as seen in Fig. 2(d). In particular, the response time of the system is decreased by almost 6 orders of magnitude during the heating period which makes it possible for  $\langle N \rangle$  to quickly reach the new equilibrium value of  $N_{\text{eq}}$ . This explains the ultrashort timescales observed in skyrmion nucleation dynamics [28]. Turning the heat pulse off instantly, in return, increases the response time of the system again by the same orders of magnitude, leading to a very slow response, effectively stopping further dynamics and freezing in the generated skyrmions.

The stabilization of non-equilibrium skyrmions after the heat pulse is only possible due to the immediate drop in temperature ( $\tau_{\text{cool}} \ll \tau_0$ ). If, instead, the cooling was quasi-adiabatic ( $\tau_{\text{cool}} \gg \tau_0$ ), the skyrmion population would always have enough time to reach the instantaneous equilibrium  $N_{\text{eq}}$  [see Fig. 2(c)] and almost all generated skyrmions would be gone when the base temperature  $T_0$  is reached. Indeed, gradually increasing the cooling time  $\tau_{\text{cool}}$  continuously decreases the final skyrmion population evaluated at  $t = 500\tau_0$ , as shown in Fig. 2(b) and Fig. 2(e). When the cooldown time becomes comparable to the response time at intermediate temperature  $T$ , a portion of the skyrmions is able to annihilate before being frozen in.

The effective theory predicts that the number of nucleation skyrmions can be directly controlled using the cooldown time of the pulse, which experimentally is feasible by engineering the heat diffusion and pulse length of the laser. For example, the metastable skyrmions considered here could be written with high and short pulses, while they could be erased with lower and wider pulse profiles as a sort of annealing, representing fully heating-based stochastic switching.

To test this hypothesis and the validity of the effective theory for time-dependent temperatures, ASD simulations were performed (using the UppASD package [55]). Such simulations were previously used to corroborate experimental results on laser-induced skyrmion nucleation [28]. In this case, the parameters of the theory are fitted from relaxation at constant temperatures. The details of this can be found in Appendix C. In ASD, one considers discrete classical magnetic moments  $\mathbf{m}_i$  in a lattice, usually the square lattice. The Hamiltonian

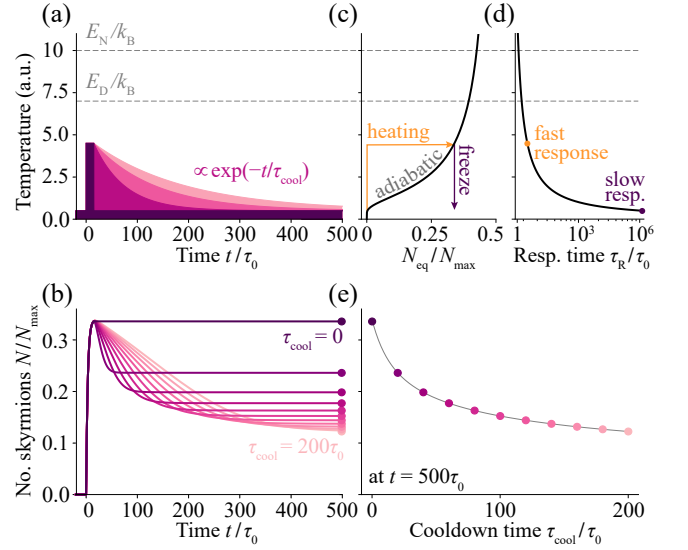


Figure 2. Calculation of heat pulse induced skyrmion nucleation dynamics  $N(t)$  using the effective theory (b) for pulses with exponential cooldown times  $\tau_{\text{cool}}$  varied between 0 and  $200\tau_0$  ((a), dark purple to light pink) after an initial constant high temperature. The final values of  $N$  from (b) are plotted as a function of cooldown time in panel (e). Temperature dependence of the equilibrium number of skyrmions  $N_{\text{eq}}$  (c) and response time  $\tau_R$  (d). The path of the rectangular pulse is illustrated with yellow and purple annotations. At high  $T$ , the response time is very short and the equilibrium number of skyrmions is enhanced, leading to nucleation. The slow response time at low  $T$  locks the system into a skyrmions state after fast cooldown, while the dynamics tend towards the adiabatic path  $N(t) = N_{\text{eq}}(T(t))$  with low final  $N$  for slower cooldown.

for the moments is given by

$$\mathcal{H}_{\text{ASD}} = - \sum_{i \neq j} J_{ij} \mathbf{m}_i \cdot \mathbf{m}_j - \sum_{i \neq j} D_{ij} (\mathbf{m}_i \times \mathbf{m}_j) - \sum_i K m_{i,z}^2 - \sum_i M \mathbf{B} \cdot \mathbf{m}_i, \quad (13)$$

which includes ferromagnetic exchange  $J_{ij} > 0$ , Dzyaloshinskii-Moriya interaction  $D_{ij}$ , uniaxial anisotropy  $K$  and the interaction with an external field  $\mathbf{B}$ . We take over the parameter set from [28] that is known to qualitatively match the experimental system, and in particular to support skyrmions. However, we increase the external field strength to  $B = 0.75$  T to ensure the homogeneous "empty" state has a lower energy than the skyrmion state as above. We use a (spatially homogeneous) exponential rise and decay on top of a base temperature  $T_0 = 4$  K to model a temperature profile induced by a laser (or current) pulse:

$$T(t) = T_0 + T_1 (1 - e^{-t/\tau_{\text{rise}}}) e^{-t/\tau_{\text{fall}}}, \quad (14)$$

with  $T_1 = c(\tau_{\text{rise}}, \tau_{\text{fall}}) T_{\text{pulse}}$ , where  $c$  is chosen such that the peak of the pulse is  $T_{\text{pulse}}$  above  $T_0$ . The parameters  $\tau_{\text{rise}}$  and  $\tau_{\text{fall}}$  control the rise time and decay time of the pulse, respectively. To test the temperature-induced writing and erasing, we apply two pulses as shown in Fig. 3(a,b) after initializing



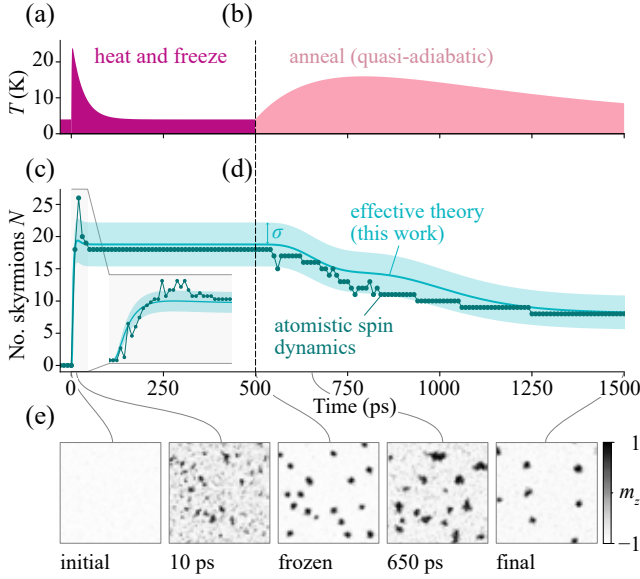


Figure 3. Prediction of (a,c) heat-induced nucleation and freezing in skyrmions by a short heat pulse and (b,d) annihilation of the same skyrmions by slow annealing and quasi-adiabatic cooldown. (a) and (b) show the temperature profile of the different heat pulses, while (c) and (d) show the resulting mean number of skyrmions  $\langle N(t) \rangle$  (with standard deviation  $\sigma$ ) as predicted by the effective theory from this work, compared with a full ASD simulation. Representative snapshots of the out-of-plane magnetization  $m_z$  from the ASD simulation are shown in panel (e).

the system in the fully field-aligned state. The first pulse has height  $T_{\text{pulse}} = 20$  K with fast heating and cooling given by  $\tau_{\text{rise}} = 1$  ps and  $\tau_{\text{fall}} = 30$  ps, while the second pulse heats and cools more slowly with  $\tau_{\text{rise}} = 300$  ps and  $\tau_{\text{fall}} = 500$  ps and reduced height  $T_{\text{pulse}} = 12$  K.

The time trace of the number of skyrmions  $N$  resulting from this temperature profile are shown for an ASD simulation (points) as well as for the effective theory (solid line and shaded area) in Fig. 3(c,d). The solid line represents the expectation value  $\langle N \rangle$  and the shaded area represents the standard deviation  $\sqrt{\text{Var}(N)}$  of the number of skyrmions calculated using the effective theory. We find excellent agreement between the curves for  $N$  for both the writing and the erasing. The dynamics of the magnetization texture in Fig. 3(e) are moreover in accordance with the assumptions and trends described by the effective theory. While the system is hot during the first pulse, skyrmions spontaneously appear (and disappear) at random places, most of which freeze in during the rapid cooldown. The second longer pulse drives the system closer to  $N_{\text{eq}}$  by allowing a random subset of skyrmions to annihilate.

**Discussion** — The current theory provides excellent agreement with ASD for the average skyrmion number. Here we only illustrate the case where the nucleation energy is higher than the decay energy, but the theory is equally applicable when skyrmions have the lowest energy ( $E_N \leq E_D$ ). Interesting extensions could be to include more skyrmion properties, for example taking into account skyrmion growth as in-

creasing stability over time [50], and space-dependent energy landscapes [56]. Beyond this, a grid-based implementation of our model can support full spatial dimensions and make it possible to reintroduce interactions between the skyrmions as well as movement. Even after such extensions, the coarse-graining drastically reduces computational costs compared to conventional micromagnetic and atomistic approaches, giving access to experimental system sizes without sacrificing expensive interactions like the long-range dipolar interaction. This paves the way to quantitative modeling of experimental ultrafast skyrmion nucleation. Furthermore, the effective theory can be generalized to other ferromagnetic systems [16, 21] and may even be applicable beyond magnetism for the description of photo-induced first-order phase transitions.

**Summary** — We have developed an effective theory of ultrafast thermally induced dynamics of the number of skyrmions. We find that skyrmions are nearly independent of each other on ultrafast timescales, allowing us to derive a simple kinetic equation for the number of skyrmions  $N(t)$  in good agreement with established atomistic models. The effective theory provides an intuitive explanation of how skyrmions can be nucleated and stabilized even when they are not the ground state. It shows non-equilibrium states are generated at elevated temperature, which can be frozen in by sufficiently fast cooldown. This also leads to a prediction that the number of nucleated skyrmions can be controlled via the cooldown rate. Given the generality of the underlying estimations, the laser-induced dynamics of magnetic textures may be more generally described by an effective theory involving nucleation and decay over energy barriers, potentially providing a unified theoretical description of a wide range of femtosecond X-ray experiments [57–61].

**Acknowledgements** — This work was funded by the European Union Horizon 2020 and innovation program under the European Research Council ERC Grant Agreement No. 856538 (3D-MAGiC). L.K. acknowledges funding by the Radboud Excellence Initiative. J.H.M. acknowledges funding by the Dutch Research Council (NWO) via VIDI project no. 223.157 (CHASEMAG) and by the EU via Horizon Europe project no. 101070290 (NIMFEIA). B.P. acknowledges funding from the Röntgen-Ångström-Cluster (Verbundprojekt 05K2024 - 2023-06359 “Soft-XPCS”). B.P. and K.G. acknowledge funding from Leibniz Association – Grant No. K162/2018 (OptiSPIN). F.B. and B.P. acknowledge funding from the Deutsche Forschungsgemeinschaft (DFG, German Research Foundation) – project number 505818345 (Topo3D). F.B. acknowledges funding from the Helmholtz Young Investigator Group Program (VH-NG-1520) and from the Deutsche Forschungsgemeinschaft – project number 49254781 (TRR360-C2).

## APPENDIX

### A. Thermal free diffusion

Here, we provide details on the Belavin-Polyakov which allows us to estimate an upper bound on the skyrmion diffusion.

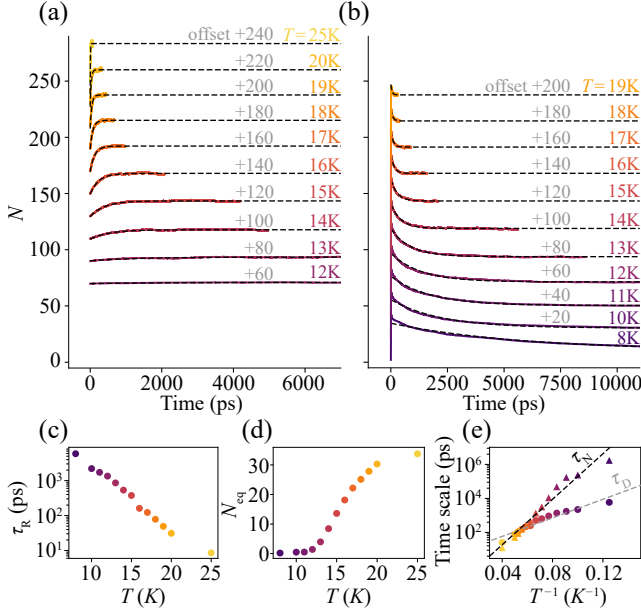


Figure 4. Fits of the ASD system at constant temperatures  $T = T_0$  to obtain effective theory parameters. Relaxation of the number of skyrmions  $N$  (average of 30 runs) at varying temperatures from a fully field-aligned (a) and fully random (b) initial state. For visibility, subsequent temperature are plotted with an offset of  $N = 20$ . The fits to Eq. (20) are shown as dashed black lines. The obtained values (weighted average from the runs with random and fully field-aligned initial state) of  $\tau_R$  (c) and  $N_{eq}$  (d) at each temperature. (e) Values for  $\tau_R$  (triangles) and  $\tau_D$  (circles) obtained from  $\tau_R$  and  $N_{eq}$  and fits with the Arrhenius law Eq. (9) (dashed lines).

Calculation of skyrmion thermal diffusion based on the Thiele equation

$$\frac{\partial \mathbf{X}}{\partial t} \times \mathbf{G} + \alpha D \frac{\partial \mathbf{X}}{\partial t} = \mathbf{F}, \quad (15)$$

is well-established [32, 40]. Without driving forces such as currents or thermal gradients, the effective forces on the right-hand side of Eq. (2) are purely stochastic, originating from thermal noise. The different Cartesian components of the thermal force are uncorrelated to each other and to themselves at different times:  $\langle F_\mu^{\text{th}}(t) F_\nu^{\text{th}}(t') \rangle = 2k_B T D \delta_{\mu\nu} \delta(t - t')$ . By writing Eq. (15) in components using  $v_x = \partial x / \partial t$  and  $v_y = \partial y / \partial t$ , one finds  $\langle v_x(t) v_x(t') \rangle = \langle v_y(t) v_y(t') \rangle = 2D \delta(t - t')$  where

$$D = k_B T \frac{\alpha_G D}{G^2 + \alpha_G^2 D^2}. \quad (16)$$

This leads to  $\langle x^2(t) \rangle = \langle y^2(t) \rangle = 2Dt$ . In the Belavin-Polyakov limit (in general  $D \geq G$ ), we have  $D = G = 4\pi\mu_0 M_s d / \gamma$  and obtain

$$D = k_B T \frac{1}{G} \frac{\alpha_G}{1 + \alpha_G^2}.$$

## B. Estimation of maximum magnon group velocity

In this section, we estimate the maximum group velocity of the magnons that can mediate long-range interactions between different skyrmions. From the scattering potentials found in [33], we can estimate that the magnon wave vectors that are relevant for magnon-skyrmion scattering are below  $2/R$  with  $R$  being the skyrmion radius. As  $R$  is typically in the order of 10 to 100 nm, we can take the continuum approach to model magnons. Moreover, for thin films, the group velocity of forward-volume waves in this range is dominated by the exchange interaction. So we can estimate

$$\omega(k) \approx C + \omega_M \lambda^2 k^2 \quad (17)$$

with  $C$  being some gap due to anisotropy and external field,  $\omega_M = \gamma\mu_0 M_s$  and  $\lambda = \sqrt{2A_{\text{ex}}/\mu_0 M_s^2}$  being the dipole-exchange length of a material with exchange stiffness  $A_{\text{ex}}$ , saturation magnetization  $M_s$  and gyromagnetic ratio  $\gamma$ . It follows that

$$\begin{aligned} v_g &= \frac{\partial \omega}{\partial k} \approx 2\omega_M \lambda^2 k \\ &= 2\gamma\mu_0 M_s \frac{2A_{\text{ex}}}{\mu_0 M_s^2} k \\ &= 4\gamma \frac{A_{\text{ex}}}{M_s} k \end{aligned} \quad (18)$$

Since  $v_g(k)$  is strictly monotonously rising, the maximum group velocity of the relevant magnons is taken at  $k = 2/R$ . Hence,

$$\max_k(v_g) = 8\gamma \frac{A_{\text{ex}}}{M_s} \frac{1}{R}. \quad (19)$$

## C. Effective parameters from atomistic spin dynamics (ASD)

Here, we extract the effective parameters of our theory by fitting it to ASD simulations of thermal relaxation. At constant temperature  $T = T_0$  the behavior of the skyrmion number  $N$  in the ASD system closely resembles exponential relaxation. This is in agreement with effective theory. We can use this to obtain an effective  $N_{eq}(T_0)$  and  $\tau_R(T_0)$  for the ASD system by fitting to

$$N(t) = N_0 + (N_{eq} - N_0) \left(1 - e^{-t/\tau_R}\right), \quad (20)$$

as shown in Fig. 4(a-d). It is not possible to directly find the maximum number of skyrmions, so we make an estimation  $N_{\text{max}} = 49$  for the  $100 \times 100$  spin system based on the size of a single skyrmions. We can now determine  $\tau_N(T_0)$  and  $\tau_D(T_0)$  through the relations  $1/\tau_R = 1/\tau_D + 1/\tau_N$  and  $N_{eq} = N_{\text{max}}\tau_R/\tau_N$ , which yield

$$\tau_N = \frac{N_{\text{max}}}{N_{eq}} \tau_C, \quad \tau_D = \frac{N_{\text{max}}}{N_{\text{max}} - N_{eq}} \tau_C. \quad (21)$$

Repeating this procedure for a range of temperatures, we can plot the temperature dependence of  $\tau_N(T)$  and  $\tau_D(T)$ . This

dependence turn out to be in reasonable agreement with the Arrhenius law Eq. (9) as seen in Fig. 4(e), allowing us find

values for  $\tau_{0,i}$  and  $E_i$  ( $i = N, D$ ) by fitting. We obtain  $\tau_{0,N} = 0.0404$  ps,  $E_N = 13.3$  meV and  $\tau_{0,D} = 4.76$  ps,  $E_D = 5.41$  meV.

- 
- [1] C. D. Stanciu, F. Hansteen, A. V. Kimel, A. Kirilyuk, A. Tsukamoto, A. Itoh, and T. Rasing, All-optical magnetic recording with circularly polarized light, *Phys. Rev. Lett.* **99**, 047601 (2007).
  - [2] A. J. Schellekens and B. Koopmans, Microscopic model for ultrafast magnetization dynamics of multisublattice magnets, *Physical Review B* **87**, 020407 (2013).
  - [3] C. Davies, T. Janssen, J. Mentink, A. Tsukamoto, A. Kimel, A. Van Der Meer, A. Stupakiewicz, and A. Kirilyuk, Pathways for Single-Shot All-Optical Switching of Magnetization in Ferrimagnets, *Physical Review Applied* **13**, 024064 (2020).
  - [4] F. Jakobs and U. Atxitia, Universal Criteria for Single Femtosecond Pulse Ultrafast Magnetization Switching in Ferrimagnets, *Physical Review Letters* **129**, 037203 (2022).
  - [5] I. Radu, K. Vahaplar, C. Stamm, T. Kachel, N. Pontius, H. A. Dürr, T. A. Ostler, J. Barker, R. F. L. Evans, R. W. Chantrell, A. Tsukamoto, A. Itoh, A. Kirilyuk, T. Rasing, and A. V. Kimel, Transient ferromagnetic-like state mediating ultrafast reversal of antiferromagnetically coupled spins, *Nature* **472**, 205 (2011).
  - [6] J. H. Mentink, J. Hellsvik, D. V. Afanasiev, B. A. Ivanov, A. Kirilyuk, A. V. Kimel, O. Eriksson, M. I. Katsnelson, and T. Rasing, Ultrafast spin dynamics in multisublattice magnets, *Phys. Rev. Lett.* **108**, 057202 (2012).
  - [7] J. Gorchon, R. B. Wilson, Y. Yang, A. Pattabi, J. Y. Chen, L. He, J. P. Wang, M. Li, and J. Bokor, Role of electron and phonon temperatures in the helicity-independent all-optical switching of gdfeco, *Phys. Rev. B* **94**, 184406 (2016).
  - [8] U. Atxitia and T. A. Ostler, Ultrafast double magnetization switching in gdfeco with two picosecond-delayed femtosecond pump pulses, *Applied Physics Letters* **113**, 062402 (2018).
  - [9] F. Steinbach, N. Stetzuh, D. Engel, U. Atxitia, C. Von Korff Schmising, and S. Eisebitt, Accelerating double pulse all-optical write/erase cycles in metallic ferrimagnets, *Applied Physics Letters* **120**, 112406 (2022).
  - [10] Y. L. W. Van Hees, B. Koopmans, and R. Lavrijsen, Toward high all-optical data writing rates in synthetic ferrimagnets, *Applied Physics Letters* **120**, 252401 (2022).
  - [11] C. E. Graves, A. H. Reid, T. Wang, B. Wu, S. De Jong, K. Vahaplar, I. Radu, D. P. Bernstein, M. Messerschmidt, L. Müller, R. Coffee, M. Bionta, S. W. Epp, R. Hartmann, N. Kimmel, G. Hauser, A. Hartmann, P. Holl, H. Gorke, J. H. Mentink, A. Tsukamoto, A. Fognini, J. J. Turner, W. F. Schlotter, D. Rolles, H. Soltau, L. Strüder, Y. Acremann, A. V. Kimel, A. Kirilyuk, T. Rasing, J. Stöhr, A. O. Scherz, and H. A. Dürr, Nanoscale spin reversal by non-local angular momentum transfer following ultrafast laser excitation in ferrimagnetic GdFeCo, *Nature Materials* **12**, 293 (2013).
  - [12] E. Iacocca, T.-M. Liu, A. H. Reid, Z. Fu, S. Ruta, P. W. Granitzka, E. Jal, S. Bonetti, A. X. Gray, C. E. Graves, R. Kukreja, Z. Chen, D. J. Higley, T. Chase, L. Le Guyader, K. Hirsch, H. Ohldag, W. F. Schlotter, G. L. Dakovski, G. Coslovich, M. C. Hoffmann, S. Carron, A. Tsukamoto, A. Kirilyuk, A. V. Kimel, T. Rasing, J. Stöhr, R. F. L. Evans, T. Ostler, R. W. Chantrell, M. A. Hoefer, T. J. Silva, and H. A. Dürr, Spin-current-mediated rapid magnon localisation and coalescence after ultrafast optical pumping of ferrimagnetic alloys, *Nature Communications* **10**, 1756 (2019).
  - [13] K. Yao, F. Steinbach, M. Borchert, D. Schick, D. Engel, F. Bencivenga, R. Mincigrucchi, L. Foglia, E. Pedersoli, D. De Angelis, *et al.*, All-optical switching on the nanometer scale excited and probed with femtosecond extreme ultraviolet pulses, *Nano Letters* **22**, 4452 (2022).
  - [14] D. Ksenzov, A. A. Maznev, V. Unikandanunni, F. Bencivenga, F. Capotondi, A. Caretta, L. Foglia, M. Malvestuto, C. Masciovecchio, R. Mincigrucchi, K. A. Nelson, M. Pancaldi, E. Pedersoli, L. Randolph, H. Rahmann, S. Urzhidn, S. Bonetti, and C. Gutt, Nanoscale Transient Magnetization Gratings Created and Probed by Femtosecond Extreme Ultraviolet Pulses, *Nano Letters* **21**, 2905 (2021).
  - [15] F. Steinbach, U. Atxitia, K. Yao, M. Borchert, D. Engel, F. Bencivenga, L. Foglia, R. Mincigrucchi, E. Pedersoli, D. De Angelis, *et al.*, Exploring the fundamental spatial limits of magnetic all-optical switching, *Nano Letters* **24**, 6865 (2024).
  - [16] C.-H. Lambert, S. Mangin, B. S. D. C. S. Varaprasad, Y. K. Takahashi, M. Hehn, M. Cinchetti, G. Malinowski, K. Hono, Y. Fainman, M. Aeschlimann, and E. E. Fullerton, All-optical control of ferromagnetic thin films and nanostructures, *Science* **345**, 1337 (2014).
  - [17] M. S. El Hadri, P. Pirro, C.-H. Lambert, S. Petit-Watelot, Y. Quessab, M. Hehn, F. Montaigne, G. Malinowski, and S. Mangin, Two types of all-optical magnetization switching mechanisms using femtosecond laser pulses, *Physical Review B* **94**, 064412 (2016).
  - [18] R. Medapalli, D. Afanasiev, D. K. Kim, Y. Quessab, S. Manna, S. A. Montoya, A. Kirilyuk, T. Rasing, A. V. Kimel, and E. E. Fullerton, Multiscale dynamics of helicity-dependent all-optical magnetization reversal in ferromagnetic Co/Pt multilayers, *Physical Review B* **96**, 224421 (2017).
  - [19] J. Gorchon, Y. Yang, and J. Bokor, Model for multishot all-thermal all-optical switching in ferromagnets, *Physical Review B* **94**, 020409 (2016).
  - [20] M. O. A. Ellis, E. E. Fullerton, and R. W. Chantrell, All-optical switching in granular ferromagnets caused by magnetic circular dichroism, *Scientific Reports* **6**, 30522 (2016).
  - [21] D. Khusyainov, R. Lieferrink, M. Na, K. Fabian, R. Frömter, M. Kläui, D. Kozodaev, N. Vovk, R. Mikhaylovskiy, D. Afanasiev, A. Kimel, J. H. Mentink, and T. Rasing, *Laser-induced helicity and texture-dependent switching of nanoscale stochastic domains in a ferromagnetic film* (2024), 2412.11700 [cond-mat].
  - [22] M. S. El Hadri, M. Hehn, P. Pirro, C.-H. Lambert, G. Malinowski, E. E. Fullerton, and S. Mangin, Domain size criterion for the observation of all-optical helicity-dependent switching in magnetic thin films, *Physical Review B* **94**, 064419 (2016).
  - [23] D. P. Gweha Nyoma, M. Hehn, G. Malinowski, J. Ghanbaja, J. Hohlfield, J. Gorchon, S. Mangin, and F. Montaigne, Gd Doping at the Co/Pt Interfaces to Induce Ultrafast All-Optical Switching, *ACS Applied Electronic Materials* **6**, 1122 (2024).
  - [24] M. Dąbrowski, S. Guo, M. Strungaru, P. S. Keatley, F. Withers, E. J. G. Santos, and R. J. Hicken, All-optical control of spin in a 2D van der Waals magnet, *Nature Communications* **13**, 5976 (2022).

- [25] K. T. Yamada, S. Ruta, A. V. Kimel, K. H. Prabhakara, T. Li, F. Ando, S. Semin, T. Ono, A. Kirilyuk, R. W. Chantrell, and T. Rasing, Ultrafast ferromagnetic spin switching by a single pair of optical pulses, *IEEE Transactions on Magnetism*, **1** (2025).
- [26] S.-G. Je, P. Vallobra, T. Srivastava, J.-C. Rojas-Sánchez, T. H. Pham, M. Hehn, G. Malinowski, C. Baraduc, S. Auffret, G. Gaudin, S. Mangin, H. Béa, and O. Boulle, Creation of magnetic skyrmion bubble lattices by ultrafast laser in ultrathin films, *Nano Letters* **18**, 7362 (2018).
- [27] G. Berruto, I. Madan, Y. Murooka, G. Vanacore, E. Pomarico, J. Rajeswari, R. Lamb, P. Huang, A. Kruchkov, Y. Togawa, T. LaGrange, D. McGrouther, H. Rønnow, and F. Carbone, Laser-induced skyrmion writing and erasing in an ultrafast cryo-lorentz transmission electron microscope, *Physical Review Letters* **120**, 117201 (2018).
- [28] F. Büttner, B. Pfau, M. Böttcher, M. Schneider, G. Mercurio, C. M. Günther, P. Hessler, C. Klose, A. Wittmann, K. Gerlinger, L.-M. Kern, C. Strüber, C. von Korff Schmising, J. Fuchs, D. Engel, A. Churikova, S. Huang, D. Suzuki, I. Lemesch, M. Huang, L. Caretta, D. Weder, J. H. Gaida, M. Möller, T. R. Harvey, S. Zayko, K. Bagschik, R. Carley, L. Mercadier, J. Schlappa, A. Yaroslavtsev, L. L. Guyard, N. Gerasimova, A. Scherz, C. Deiter, R. Gort, D. Hickin, J. Zhu, M. Turcato, D. Lomidze, F. Erdinger, A. Castoldi, S. Maffessanti, M. Porro, A. Samartsev, J. Sinova, C. Ropers, J. H. Mentink, B. Dupé, G. S. D. Beach, and S. Eisebitt, Observation of fluctuation-mediated picosecond nucleation of a topological phase, *Nature Materials* **20**, 30 (2020).
- [29] K. Gerlinger, R. Lieferrink, M. Schneider, L.-M. Kern, C. Klose, D. Metternich, D. Engel, F. Capotondi, D. De Angelis, M. Pancaldi, E. Pedersoli, F. Büttner, S. Eisebitt, J. H. Mentink, and B. Pfau, *Robust scenario for the generation of non-equilibrium topological fluctuation states* (2022).
- [30] Z. Li, H. Zhang, G. Li, J. Guo, Q. Wang, Y. Deng, Y. Hu, X. Hu, C. Liu, M. Qin, X. Shen, R. Yu, X. Gao, Z. Liao, J. Liu, Z. Hou, Y. Zhu, and X. Fu, Room-temperature sub-100 nm Néel-type skyrmions in non-stoichiometric van der Waals ferromagnet Fe<sub>3</sub>-xGaTe<sub>2</sub> with ultrafast laser writability, *Nature Communications* **15**, 1017 (2024).
- [31] A. A. Thiele, Steady-state motion of magnetic domains, *Phys. Rev. Lett.* **30**, 230 (1973).
- [32] M. Weisshofer, L. Rózsa, and U. Nowak, Skyrmion dynamics at finite temperatures: Beyond thiele's equation, *Phys. Rev. Lett.* **127**, 047203 (2021).
- [33] C. Schütte and M. Garst, Magnon-skyrmion scattering in chiral magnets, *Phys. Rev. B* **90**, 094423 (2014).
- [34] F. Büttner, C. Moutafis, M. Schneider, B. Krüger, C. M. Günther, J. Geilhufe, C. Schmising, J. Mohanty, B. Pfau, S. Schaffert, A. Bisig, M. Foerster, T. Schulz, C. A. F. Vaz, J. H. Franken, H. J. M. Swagten, M. Kläui, and S. Eisebitt, Dynamics and inertia of skyrmionic spin structures, *Nature Physics* **11**, 225 (2015).
- [35] R. Gruber, J. Zázvorka, M. A. Brems, D. R. Rodrigues, T. Dohi, N. Kerber, B. Seng, M. Vafaei, K. Everschor-Sitte, P. Virnau, and M. Kläui, Skyrmion pinning energetics in thin film systems, *Nature Communications* **13**, 3144 (2022).
- [36] J. Zázvorka, F. Jakobs, D. Heinze, N. Keil, S. Kromin, S. Jaiswal, K. Litzius, G. Jakob, P. Virnau, D. Pinna, K. Everschor-Sitte, L. Rózsa, A. Donges, U. Nowak, and M. Kläui, Thermal skyrmion diffusion used in a reshuffler device, *Nature Nanotechnology* **14**, 658 (2019).
- [37] M. A. Brems, T. Sparmann, S. M. Fröhlich, L.-C. Dany, J. Rothörl, F. Kammerbauer, E. M. Jefremovas, O. Farago, M. Kläui, and P. Virnau, Realizing quantitative quasiparticle modeling of skyrmion dynamics in arbitrary potentials, *Phys. Rev. Lett.* **134**, 046701 (2025).
- [38] F. Büttner, I. Lemesch, and G. S. D. Beach, Theory of isolated magnetic skyrmions: From fundamentals to room temperature applications, *Scientific Reports* **8**, 10.1038/s41598-018-22242-8 (2018).
- [39] J. Sampaio, V. Cros, S. Rohart, A. Thiaville, and A. Fert, Nucleation, stability and current-induced motion of isolated magnetic skyrmions in nanostructures, *Nature Nanotechnology* **8**, 839 (2013).
- [40] J. Miltat, S. Rohart, and A. Thiaville, Brownian motion of magnetic domain walls and skyrmions, and their diffusion constants, *Phys. Rev. B* **97**, 214426 (2018).
- [41] A. A. Belavin and A. M. Polyakov, Metastable states of two-dimensional isotropic ferromagnets, *JETP Letters* **22** (1975).
- [42] J. Wild, T. N. G. Meier, S. Pöllath, M. Kronseder, A. Bauer, A. Chacon, M. Halder, M. Schowalter, A. Rosenauer, J. Zweck, J. Müller, A. Rosch, C. Pfleiderer, and C. H. Back, Entropy-limited topological protection of skyrmions, *Science Advances* **3**, 10.1126/sciadv.1701704 (2017).
- [43] J. Tang, J. Jiang, Y. Wu, L. Kong, Y. Wang, J. Li, Y. Soh, Y. Xiong, S. Wang, M. Tian, and H. Du, Creating and Deleting a Single Dipolar Skyrmion by Surface Spin Twists, *Nano Letters* **25**, 121 (2025).
- [44] A. Bernand-Mantel, C. B. Muratov, and V. V. Slastikov, A micromagnetic theory of skyrmion lifetime in ultrathin ferromagnetic films, *Proceedings of the National Academy of Sciences* **119**, e2122237119 (2022), <https://www.pnas.org/doi/pdf/10.1073/pnas.2122237119>.
- [45] S.-G. Je, D. Thian, X. Chen, L. Huang, D.-H. Jung, W. Chao, K.-S. Lee, J.-I. Hong, A. Soumyanarayanan, and M.-Y. Im, Targeted Writing and Deleting of Magnetic Skyrmions in Two-Terminal Nanowire Devices, *Nano Letters* **21**, 1253 (2021).
- [46] A. D. Verga, Skyrmion to ferromagnetic state transition: A description of the topological change as a finite-time singularity in the skyrmion dynamics, *Physical Review B* **90**, 174428 (2014).
- [47] L. Rózsa, E. Simon, K. Palotás, L. Udvardi, and L. Szunyogh, Complex magnetic phase diagram and skyrmion lifetime in an ultrathin film from atomistic simulations, *Physical Review B* **93**, 024417 (2016).
- [48] J. Wang, M. Strungaru, S. Ruta, A. Meo, Y. Zhou, A. Deák, L. Szunyogh, P.-I. Gavriloea, R. Moreno, O. Chubykalo-Fesenko, J. Wu, Y. Xu, R. F. L. Evans, and R. W. Chantrell, Spontaneous creation and annihilation dynamics of magnetic skyrmions at elevated temperature, *Physical Review B* **104**, 054420 (2021).
- [49] P. Olleros-Rodríguez, M. Strungaru, S. Ruta, P.-I. Gavriloea, A. Gudiñ, P. Perna, R. Chantrell, and O. Chubykalo-Fesenko, Non-equilibrium heating path for the laser-induced nucleation of metastable skyrmion lattices, *Nanoscale* **14**, 15701 (2022).
- [50] P. F. Bessarab, G. P. Müller, I. S. Lobanov, F. N. Rybakov, N. S. Kiselev, H. Jónsson, V. M. Uzdin, S. Blügel, L. Bergqvist, and A. Delin, Lifetime of racetrack skyrmions, *Scientific Reports* **8**, 10.1038/s41598-018-21623-3 (2018).
- [51] P. F. Bessarab, V. M. Uzdin, and H. Jónsson, Method for finding mechanism and activation energy of magnetic transitions, applied to skyrmion and antivortex annihilation, *Computer Physics Communications* **196**, 335 (2015).
- [52] L. Desplat, J.-V. Kim, and R. L. Stamps, Paths to annihilation of first- and second-order (anti)skyrmions via (anti)meron nucleation on the frustrated square lattice, *Physical Review B* **99**, 174409 (2019).



- [53] L. Desplat, D. Suess, J.-V. Kim, and R. L. Stamps, Thermal stability of metastable magnetic skyrmions: Entropic narrowing and significance of internal eigenmodes, *Physical Review B* **98**, 134407 (2018).
- [54] M. Hoffmann, G. P. Müller, and S. Blügel, Atomistic Perspective of Long Lifetimes of Small Skyrmions at Room Temperature, *Physical Review Letters* **124**, 247201 (2020).
- [55] B. Skubic, J. Hellsvik, L. Nordström, and O. Eriksson, A method for atomistic spin dynamics simulations: implementation and examples, *Journal of Physics: Condensed Matter* **20**, 315203 (2008).
- [56] L.-M. Kern, B. Pfau, V. Deinhart, M. Schneider, C. Klose, K. Gerlinger, S. Wittrock, D. Engel, I. Will, C. M. Günther, R. Liefferink, J. H. Mentink, S. Wintz, M. Weigand, M.-J. Huang, R. Battistelli, D. Metternich, F. Büttner, K. Höflich, and S. Eisebitt, Deterministic generation and guided motion of magnetic skyrmions by focused  $\text{He}^+$ -ion irradiation, *Nano Letters* **22**, 4028 (2022).
- [57] C. von Korff Schmising, B. Pfau, M. Schneider, C. M. Günther, M. Giovannella, J. Perron, B. Vodungbo, L. Müller, F. Capotondi, E. Pedersoli, N. Mahne, J. Lüning, and S. Eisebitt, Imaging ultrafast demagnetization dynamics after a spatially localized optical excitation, *Phys. Rev. Lett.* **112**, 217203 (2014).
- [58] Y. Guang, I. Bykova, Y. Liu, G. Yu, E. Goering, M. Weigand, J. Gräfe, S. K. Kim, J. Zhang, H. Zhang, *et al.*, Creating zero-field skyrmions in exchange-biased multilayers through x-ray illumination, *Nature communications* **11**, 949 (2020).
- [59] S. Zayko, O. Kfir, M. Heigl, M. Lohmann, M. Sivilis, M. Albrecht, and C. Ropers, Ultrafast high-harmonic nanoscopy of magnetization dynamics, *Nature communications* **12**, 6337 (2021).
- [60] M. Khela, M. Dąbrowski, S. Khan, P. S. Keatley, I. Verzhbitskiy, G. Eda, R. J. Hicken, H. Kurebayashi, and E. J. Santos, Laser-induced topological spin switching in a 2d van der waals magnet, *Nature communications* **14**, 1378 (2023).
- [61] R. Battistelli, D. Metternich, M. Schneider, L.-M. Kern, K. Litzius, J. Fuchs, C. Klose, K. Gerlinger, K. Bagschik, C. M. Günther, *et al.*, Coherent x-ray magnetic imaging with 5 nm resolution, *Optica* **11**, 234 (2024).